

Dynamical magneto-electric coupling in helical magnets

Hosho Katsura,^{1,*} Alexander V. Balatsky,^{2,†} and Naoto Nagaosa^{1,3,4,‡}

¹*Department of Applied Physics, the University of Tokyo,
7-3-1, Hongo, Bunkyo-ku, Tokyo 113-8656, Japan*

²*Theoretical Division, Los Alamos National Laboratory, Los Alamos, New Mexico 87545 USA*

³*Correlated Electron Research Center (CERC), National Institute of Advanced Industrial
Science and Technology (AIST), Tsukuba Central 4, Tsukuba 305-8562, Japan*

⁴*CREST, Japan Science and Technology Agency (JST), Japan*

Collective mode dynamics of the helical magnets coupled to electric polarization via spin-orbit interaction is studied theoretically. The soft modes associated with the ferroelectricity are not the transverse optical phonons, as expected from the Lyddane-Sachs-Teller relation, but are the spin waves hybridized with the electric polarization. This leads to the Drude-like dielectric function $\epsilon(\omega)$ in the limit of zero magnetic anisotropy. There are two more low-lying modes; phason of the spiral and rotation of helical plane along the polarization axis. The roles of these soft modes in the neutron scattering and antiferromagnetic resonance are revealed, and a novel experiment to detect the dynamical magneto-electric coupling is proposed.

PACS numbers: 73.43.-f, 72.25.Dc, 72.25.Hg, 85.75.-d

The gigantic coupling between the magnetism and ferroelectric properties is now an issue of keen interest [1, 2, 3, 4, 5, 6, 7, 8, 9]. A representative system of interest is $RMnO_3$ with $R=Gd, Tb, Dy$. For example, $TbMnO_3$ shows a ferroelectric moment $P//c$ below a temperature $T_{FE} = 28K (< T_{Neel} = 42)$, and furthermore changes its direction of electric polarization to a axis under the magnetic field $H//b$ [1, 2, 3, 4]. Similar strong coupling behavior has been observed in $Ni_3V_2O_8$ [5], RMn_2O_5 ($R=Tb, Ho, Dy$) [6, 7], $Ba_{0.5}Sr_{1.5}Zn_2Fe_{12}O_{22}$ [8]. A common and essential feature of these compounds is that there are frustrations in the magnetic interactions. For $RMnO_3$, Kimura *et al.* [2] revealed that the increased $GdFeO_3$ -type distortion of perovskite lattice leads to the further-neighbor exchange interactions and nontrivial magnetic structures. Later the neutron scattering experiment determined the spin structure of $TbMnO_3$; it shows the incommensurate collinear spin ordering pointing along b -direction for $T_{FE} < T < T_{Neel}$, while the helical spin structure winding within the $b-c$ plane occurs for $T < T_{FE}$ with the helical wave vector $q//b$ [9]. A similar helical structure is also observed in $Ni_3V_2O_8$ [5]. These experiments point to key role of the non-collinear spin configurations such as helical spin structure, which are induced by frustrated exchange interactions, in producing the electric polarization and enhanced magneto-electric coupling.

A microscopic mechanism of the ferroelectricity of magnetic origin has recently been proposed by Katsura *et al.* [10], which is based on the idea that spin current is induced between the noncollinear spins and hence is the electric moment due to Aharonov-Casher effect [11, 12]. This result can be regarded as an inverse effect of Dzyaloshinskii-Moriya interaction [13]. Phenomenological treatment of this mechanism [14] and its extension to include electron-lattice interaction [15] have been also

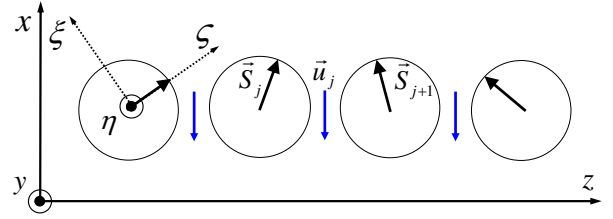


FIG. 1: Schematic ground state configuration of spins (black arrows) and lattice displacements (blue arrows).

reported. By now the static and/or ground state properties of the magneto-electric coupled systems are well understood. The obvious next step is to study their novel dynamic properties searching for the unique electromagnetic effects. In this context, we recall that the collective modes are a central issue in the research on ferroelectrics, where one of the transverse optical (TO) phonons softens toward the phase transition and is condensed according to the Lyddane-Sachs-Teller relation. This conventional view is not relevant in the case of multiferroics since the lattice displacement is not essential to the electronic polarization. Therefore it is an important open problem to identify relevant collective mode that are responsible for ferroelectricity of magnetic origin.

In this paper, we study exactly this question, i.e., the low energy dynamics of the system of the coupled spins and electric polarization. We found the new collective modes of spin and polarization waves that couple the dielectric and magnetic properties in a novel way. Experiments aimed at the detection of these collective modes in terms of the magnetic resonance, neutron scattering and the ac-dielectric measurement are also discussed.

In ref. [10], Katsura *et al.* have shown that spin (super)current in noncollinear magnets $\vec{j}_s (\propto \vec{S}_i \times \vec{S}_j)$ leads

to the electric polarization $\vec{P} \propto \vec{e}_{ij} \times \vec{j}_s$ with \vec{e}_{ij} being the unit vector connecting two sites i and j . An effective Hamiltonian describing this coupling between the spins and the atomic displacement \vec{u}_i , which represents the electric polarization including the displacement of electronic cloud, is given as;

$$H = H_1 + H_2 + H_3 + H_4, \quad (1)$$

$$H_1 = - \sum_{m,n} J(R_m - R_n) \vec{S}_m \cdot \vec{S}_n, \quad (2)$$

$$H_2 = -\lambda \sum_m (\vec{u}_m \times \vec{e}_z) \cdot (\vec{S}_m \times \vec{S}_{m+1}), \quad (3)$$

$$H_3 = \sum_m \left(\frac{\kappa}{2} \vec{u}_m^2 + \frac{1}{2M} \vec{P}_m^2 \right), \quad (4)$$

$$H_4 = \sum_m D(S_m^y)^2. \quad (5)$$

Here, the spin-lattice interaction λ stems from the relativistic spin-orbit interaction and corresponds to the DM interaction once the static displacement $\langle \vec{u}_j \rangle$ is non-zero and breaks the inversion symmetry. Note that purely electronic polarization is possible even without the atomic displacement, but the latter is always accompanied with the inversion symmetry breaking. Therefore \vec{u}_m should be regarded as the lowest frequency representative coordinates relevant to the polarization, i.e., the transverse optical phonon, and the polarization \vec{p} is given by $e^* \vec{u}_m$ with a Born charge e^* . The term $D(S^y)^2$ with positive D represents the easy-plane spin anisotropy. Here, we have assumed that the ground state spin configuration on the plane perpendicular to the helical wave vector is ferromagnetic and the low-energy excitations on this plane have a usual parabolic dispersion relation, i.e., $\propto |\vec{q}_\perp|^2$. Hence we shall focus on the modes along the helical wave vector which is set parallel to the z -axis shown in Fig.1. In H_1 , the summation is taken over all the combinations of m, n and $J(R_m - R_n)$ denotes the Heisenberg interaction between \vec{S}_m and \vec{S}_n at R_m and R_n , respectively. First, we determine the classical ground state configuration of spins and lattice distortions. Since we consider the static configuration, the kinetic term in H_3 can be negligible. The variation of H with respect to \vec{u}_m gives $\vec{u}_m = \frac{\lambda}{\kappa} \vec{e}_z \times (\vec{S}_m \times \vec{S}_{m+1})$. Henceforth we assume that spins are on the easy plane, i.e., zx -plane and explicitly given by $S_n^z = S \cos(QR_n + \phi)$, $S_n^x = S \sin(QR_n + \phi)$, $S_n^y = 0$. By substituting this spin configuration into the energy ε per spin is rewritten as $\varepsilon = -S^2 \tilde{J}(Q)$ with $\tilde{J}(q) \equiv J(q) + \frac{\lambda^2 S^2}{2\kappa} \sin^2(qa)$. Here $J(q) \equiv \sum_m J(R_m) e^{-iqR_m}$ is the Fourier transform of $J(R_m)$ and a denotes the lattice constant. The wave number Q is determined to maximize $\tilde{J}(q)$. Using Q , the uniform lattice displacement is given as $\vec{u}_m = -\frac{\lambda S^2}{\kappa} \sin(Qa) \vec{e}_x$, and hence the static electric polarization is given as $\vec{p} = -p \vec{e}_x$ with $p = e^* u_m^x = e^* \frac{\lambda S^2}{\kappa} \sin(Qa)$.

Now we consider the equations of motion for spins and

displacements, and study the collective modes of our system. We introduce a rotating local coordinate system ξ, η, ζ such that the ζ -axis coincides with the equilibrium spin direction at each site, the ξ -axis is perpendicular to this direction in zx -plane and the η -axis parallel to the y -axis (see Fig.1) [16]. Assuming the small quantum/thermal fluctuations around the classical configuration, S_n^ζ and u_n^x can be regarded as a constant and the equation of motion can be written as $\dot{S}_n^\xi = S_n^\eta H_n^\zeta - S H_n^\eta$, $\dot{S}_n^\eta = S H_n^\xi - S_n^\xi H_n^\zeta$, where $S = S_n^\zeta = \text{const.}$, and $\vec{H}_n = (H_n^\xi, H_n^\eta, H_n^\zeta)$ is the effective field acting on the n -th spin explicitly given by

$$\begin{cases} H_n^\zeta = 2S \left(J(Q) + \frac{\lambda^2 S^2}{\kappa} \sin^2(Qa) \right) \\ H_n^\xi = \sum_m 2J(R_m - R_n) S_m^\xi \cos(Q(R_m - R_n)) \\ \quad + \frac{\lambda^2 S^2}{\kappa} \sin^2(Qa) (S_{n+1}^\xi + S_{n-1}^\xi) \\ H_n^\eta = \sum_m 2J(R_m - R_n) S_m^\eta - 2D S_n^\eta \\ \quad + \lambda S (u_n^y \cos(QR_{n+1} + \phi) - u_{n-1}^y \cos(QR_{n-1} + \phi)) \end{cases} \quad (6)$$

Here, we regard S^ξ, S^η and u^y as sufficiently small and neglect their second- or higher order terms. We can also write down the equation of motion for u^y . Introducing the Fourier components of S_m^ξ, S_m^η, u_m^y and p_m^y , the equations of motion are given by

$$\begin{aligned} \dot{S}_q^\eta &= -A(q) S_q^\xi, \\ \dot{S}_q^\xi &= B(q) S_q^\eta - i\lambda S^2 \left(\frac{e^{iQa} - e^{-iqa}}{2i} e^{i\phi} u_{q-Q} + \left(\begin{smallmatrix} Q \rightarrow -Q \\ \phi \rightarrow -\phi \end{smallmatrix} \right) \right), \\ \dot{u}_q &= \frac{1}{M} p_q, \\ \dot{p}_q &= -\kappa u_q + i\lambda S \left(\frac{e^{iQa} - e^{i(q-Q)a}}{2i} e^{i\phi} S_{q-Q}^\eta + \left(\begin{smallmatrix} Q \rightarrow -Q \\ \phi \rightarrow -\phi \end{smallmatrix} \right) \right), \end{aligned} \quad (7)$$

where

$$\begin{aligned} A(q) &= 2S \left[J(Q) - \frac{J(Q+q) + J(Q-q)}{2} \right. \\ &\quad \left. + \frac{2\lambda^2 S^2}{\kappa} \sin^2(qa/2) \sin^2(Qa) \right], \\ B(q) &= 2S \left[J(Q) - J(q) + \frac{\lambda^2 S^2}{\kappa} \sin^2(Qa) + D \right]. \end{aligned} \quad (8)$$

We note that $A(q)$ and $B(q)$ satisfy the relations $A(-q) = A(q)$, $B(-q) = B(q)$, respectively, and $A(0)$ is equal to zero.

From Eq.(7), one can see the coupling between the spin wave modes and electric polarization. First S^η and S^ξ are canonical conjugate variables, and form a harmonic oscillator at each q in the rotated frame. This spin wave at q is coupled with the phonon u at $q \pm Q$, or u_q is coupled to

S^η/S^ξ at $q \pm Q$. Especially the uniform lattice displacement u_0^y is coupled to $e^{-i\phi}S_Q^\alpha - e^{i\phi}S_{-Q}^\alpha$ ($\alpha = \eta, \xi$), which corresponds to the rotation of both the spin plane and the direction of the polarization along the z -axis. This mode is the Goldstone boson with frequency $\omega = 0$ when $D = 0$, i.e., the symmetric case around z -axis. On the other hand, $e^{-i\phi}S_Q^\alpha + e^{i\phi}S_{-Q}^\alpha$ corresponds to the rotation of spin plane along x -axis, which is decoupled to the polarization but is gapped by the effective spin anisotropy introduced by the spin-lattice interaction. The spin wave mode at $q = 0$ corresponds to the sliding mode, i.e., phason, of the spiral. This is decoupled from u and has zero energy at $q = 0$.

Using Eq.(7) with canonical commutation relations $[u_q, p_{q'}] = i\delta_{q,-q'}$ and $[S_q^\xi, S_{q'}^\eta] = iS\delta_{q,-q'}$, the matrix form of the retarded Green's function

$$\begin{aligned} G^R(AB; t - t') &\equiv -i\theta(t - t')\langle [A(t), B(t')] \rangle, \\ G^R(AB; \omega) &\equiv \frac{1}{2\pi} \int_{-\infty}^{\infty} G_{AB}^R(t) e^{i\omega t}, \end{aligned} \quad (9)$$

($A, B = u_q, p_q, S_q^\xi, S_q^\eta$) is obtained. The imaginary part of the ac susceptibility is also defined as $\chi''(AB; \omega) \equiv -\text{Im}G^R(AB; \omega)$. To be more explicit, we will discuss below some physically important cases.

ac dielectric properties – The dynamical dielectric function is given by $\varepsilon_{yy}(\omega) = 1 + 4\pi(e^*)^2 G^R(u_0 u_0; \omega)$, where the e^* is the Born charge corresponding to the displacement u^y along y -axis, and

$$G^R(u_0 u_0; \omega) = \frac{\omega^2 - \omega_p^2}{2\pi M(\omega^4 - (\omega_0^2 + \omega_p^2)\omega^2 + A(Q)D\omega_0^2)}, \quad (10)$$

where $\omega_p = \sqrt{A(Q)B(Q)}$ is the frequency of the spin-plane rotation mode along x -axis, i.e., $e^{-i\phi}S_Q^\alpha + e^{i\phi}S_{-Q}^\alpha$, and $\omega_0 = \sqrt{\kappa/M}$ is that for the original phonon. This response function has the poles at ω_\pm , which are explicitly given by

$$\omega_\pm^2 = \frac{1}{2} \left(\omega_0^2 + \omega_p^2 \pm \sqrt{(\omega_0^2 + \omega_p^2)^2 - 4A(Q)D\omega_0^2} \right) \quad (11)$$

Assuming $D, \lambda \ll \omega_0^2$, one can estimate as $\omega_- \cong \sqrt{A(Q)D} \sim \sqrt{8SJ D}$, and $\omega_+ \cong \omega_0$. With this frequencies, one can write $\varepsilon_{yy}(\omega) = 1 + \sum_{\pm} \omega_{\pm} I_{\pm} / (\omega^2 - \omega_{\pm}^2)$ with the “oscillator strengths” I_{\pm} being given by $I_- = 2(e^*)^2(\omega_p^2 - \omega_-^2) / (M\omega_-(\omega_+^2 - \omega_-^2))$, and $I_+ = 2(e^*)^2(\omega_+^2 - \omega_p^2) / (M\omega_+(\omega_+^2 - \omega_-^2))$. Note that the integral $-\int_0^\infty d\omega \varepsilon_{yy}(\omega)$ is given by $(\pi/2)(I_- + I_+)$. Here, the two modes contributing to the dielectric function are (i) the phonon mode with the frequency $\omega_+ \cong \omega_0$, and (ii) the z -axis rotation mode at $\omega_- \cong \sqrt{A(Q)D}$. Usually ω_0 is a high frequency and does not show any softening in the present case. The ferroelectricity is due to the spin ordering, which is hybridized with the polarization mode. In other words, the low frequency dielectric function is mostly due to the spin wave mode at $\pm Q$.

Note the low-frequency behavior of $\varepsilon_{yy}(\omega)$ is similar to the Drude form when $D = 0$, and the oscillator strength I_- (at $\omega = \omega_-$) is enhanced as $I_- \sim p^2 \sqrt{J/D}$ as $D \rightarrow 0$. This means that even though the spin-polarization coupling λ and hence the static polarization p is small, the spin wave mode can contribute significantly when D is small.

neutron scattering spectra – Next, we shall examine how the spin-polarization coupling affects the (inelastic) neutron scattering spectra. The intensity of the neutron scattered with the momentum transfer q is estimated as

$\frac{d^2\sigma}{d\Omega d\omega} \propto -\text{Im} \sum_{\alpha \in \perp} G^R(S_q^\alpha S_{-q}^\alpha; \omega)$, where the superscript α indicates the components perpendicular to \vec{q} . In what follows, for the sake of simplicity, we set $D = 0, \phi = 0$. In order to study the neutron scattering spectra, it is needed to rotate the spin coordinates back to the original laboratory system S^a ($a = x, y, z$). We can easily derive the transformation formula given by

$$\begin{cases} G^R(S_q^x S_{-q}^x; \omega) = \frac{1}{4} \sum_{\substack{p=\pm Q \\ p'=\pm Q}} G^R(S_{q+p}^\xi S_{-q-p'}^\xi; \omega), \\ G^R(S_q^y S_{-q}^y; \omega) = G^R(S_q^\eta S_{-q}^\eta; \omega), \\ G^R(S_q^z S_{-q}^z; \omega) = \frac{1}{4} \sum_{\substack{p=\pm Q \\ p'=\pm Q}} \text{sgn}(pp') G^R(S_{q+p}^\xi S_{-q-p'}^\xi; \omega). \end{cases} \quad (12)$$

For example, at the helical wavevector $\vec{q} = (0, 0, Q)$, one can read the neutron scattering spectra by using the above transformation formula (12) and the list of pole positions and corresponding intensities summarized in Table I(a) and (b). Note that the Green's function is written as $G^R(\omega) = \sum_i a_i / (\omega^2 - \omega_i^2)$ using the intensity a_i and the pole position ω_i . Now 4 modes are expected to contribute to the neutron spectrum [17]; (i) phason mode at $\omega = 0$, (ii) x -axis rotation mode at $\omega = \omega_p$, (iii) phonon mode with $q = 0$ at $\omega = \sqrt{\omega_0^2 + \omega_p^2}$, and (iv) phonon mode with $q = Q$ at ω_0 . The former two, i.e., (i) and (ii), are of magnetic origin, and can be detected without the spin-polarization coupling, while the weights of the latter two, i.e., (iii) and (iv), are borrowed from the spin wave, and hence their relative magnitudes to the former ones are roughly estimated as; (iii)/(i) $\sim (\omega_p/\omega_0)^2$, and (iv)/(i) $\sim \lambda^2/(\kappa J)$.

antiferromagnetic resonance – We shall briefly discuss the antiferromagnetic resonance in our system. Here, $D = 0$, and $\phi = 0$ are also assumed. Magnetic resonance experiments pick up uniform magnetic excitations and corresponding Green's functions are $G^R(S_0^a S_0^a; \omega)$, ($a = x, y, z$), where axis a corresponds to the direction of applying oscillating magnetic field. Using again the transformation formula (12), one can see the pole of $G^R(S_0^x S_0^x; \omega)$ occurs at $\omega = \omega_p$ with the intensity $SB(Q)/(4\pi)$, while that of $G^R(S_0^z S_0^z; \omega)$ at $\omega =$

(a) $G^R(S_Q^y S_{-Q}^y; \omega)$			
ω_i	0	ω_p	$\sqrt{\omega_0^2 + \omega_p^2}$
a_i	$\frac{SA(Q)}{4\pi} \frac{\omega_0^2}{\omega_0^2 + \omega_p^2}$	$\frac{SA(Q)}{4\pi}$	$\frac{SA(Q)}{4\pi} \frac{\omega_p^2}{\omega_0^2 + \omega_p^2}$

(b) $G^R(S_Q^x S_{-Q}^x; \omega) = G^R(S_Q^z S_{-Q}^z; \omega)$	
ω_i	0
a_i	$\frac{S}{8\pi} \left(B(0) - \frac{2\lambda^2 S^3}{\kappa} \sin^2 \left(\frac{Qa}{2} \right) \right)$

TABLE I: The pole positions ω_i and corresponding intensities a_i for each Green's function.

$\sqrt{\omega_0^2 + \omega_p^2}$ with the intensity $SB(Q)/(4\pi)$. Note here that there is no dynamics of S_0^y since it is a conserved quantity. The phonon mode with $q = \pm Q$ has a high frequency $\omega = \sqrt{\omega_0^2 + \omega_p^2}$ and should be difficult to be observed experimentally. The x -axis rotation mode of low frequency ($\omega = \omega_p$) is not coupled directly to the polarization, while the resonance intensity is due to the spin anisotropy induced by the spin-lattice coupling λ and/or the spin anisotropy D as discussed earlier [18].

Now we turn to the realistic estimation of the parameters in our theory extracted from the experiments on $RMnO_3$. The exchange coupling constant can be estimated from the spin wave dispersion observed in the neutron scattering experiment [19]. They estimated the exchange coupling J_1 between the nearest neighbor spins as $8SJ_1 \cong 9$ meV for $PrMnO_3$ and $8SJ_1 \cong 2.4$ meV for $TbMnO_3$. On the other hand, the anisotropy energy, which corresponds to D in our theory, is around 0.4 meV for both compounds. From the ESR spectra of Jahn-Teller distorted $LaMnO_{3+\delta}$ ($0 \leq \delta \leq 0.07$), Dzyaloshinskii-Moriya coupling is estimated as $\mathcal{D} \sim 0.1$ meV [20] and hence we can evaluate the spin-lattice coupling $\lambda \sim 1$ meV/Å [15]. Assuming $\kappa \sim 1$ eV/Å² [15], we can obtain the static displacement $u_m = 10^{-3}$ Å. Another important quantity is the Born charge e^* . This can be estimated from the value of electric polarization with the above u_m and the lattice constant $a \sim 5$ Å. The electric polarization along c -axis is determined as $P_c \sim 0.2$ μC/cm² for $DyMnO_3$ [3] and hence we can estimate the Born charge e^* as $16e$ where e is the bare unit charge. This result, i.e., the Born charge is much greater than the unit charge, indicates that the electric polarization mainly consists of the displacement of the electronic cloud. At this moment, let us check the consistency of our estimation with another recent experiment on dielectric response [21]. They observed the peak of $\text{Im}\epsilon$ at around 20cm^{-1} with the magnitude of $1 \sim 2$ in $GdMnO_3$ and $TbMnO_3$. This 20cm^{-1} is identified with ω_- in Eq.(12), and the integration of $-\text{Im}\epsilon_{yy}(\omega)$ over ω gives the "oscillator strength" $(\pi/2)I_-$. From their results, we can estimate $I_- \sim 12\text{cm}^{-1}$. On the other hand, ω_- and I_- are independently estimated as $\omega_- \sim 10\text{cm}^{-1}$

and $I_- \sim 4\text{cm}^{-1}$ from the parameters determined above. Here, we have assumed that $S = 2$ and $Qa = \pi/4$. Both ω_- 's and I_- 's, are of the same order and hence we can conclude that our phenomenological model well describes the magneto-electric coupling in $RMnO_3$. It turned out that the coupling between the spin wave and the transverse phonon is weak, and is characterized by the ratio $\lambda^2/(\kappa J) \sim 10^{-3}$. Therefore, it would be rather difficult to see this coupling in the neutron scattering experiment, i.e., the magnetic scattering by the phonon modes. However, note that the low energy dielectric response reflects the spin wave mode as the Goldstone boson, i.e., z -axis spin rotation mode, and it would be enhanced more if the spin anisotropy is weaker.

Lastly, we propose a novel experiment to see directly the dynamical magneto-electric coupling. Namely we can excite the spin wave by electric field. These responses are described by the off-diagonal element of the Green's function;

$$G^R(u_0^y S_0^z; \omega) = -G^R(S_0^z u_0^y; \omega) = \frac{1}{2\pi M} \frac{i\lambda S^2 \sin(Qa)\omega}{\omega^4 - (\omega_0^2 + \omega_p^2)\omega^2 + A(Q)D\omega_0^2}. \quad (13)$$

Proposed experiment requires to put the sample between the two electrodes and apply the a.c. electric field E_y of frequency ω along y -direction. Then the magnetization of the same frequency ω can be detected at the edges of the sample polarized along z -direction. Now $\omega_- \cong 20\text{cm}^{-1}$ corresponds to the Tera-Hertz region, and the highest intensity of the electric field there is $\sim 10^3$ V/cm. Putting this value and all the other parameters estimated above with overdamping $\gamma \sim \omega_- = 20\text{cm}^{-1}$, we obtain the estimation for the magnitude of the a.c. magnetization as $m^z \sim 0.4 \times 10^{-4} \mu_B/\text{Mn atom}$, which can be detected by Kerr rotation spectroscopy. We should note here that the magnitude of m^z is much enhanced when γ is small.

The authors are grateful to T. Arima, Y. Tokura, R. Kajimoto, T. Kimura and T. Lookman for fruitful discussions. This work is financially supported by NAREGI Grant, Grant-in-Aids from the Ministry of Education, Culture, Sports, Science and Technology of Japan and by the US Department of Energy.

* Electronic address: katsura@appi.t.u-tokyo.ac.jp

† Electronic address: avb@lanl.gov

‡ Electronic address: nagaosa@appi.t.u-tokyo.ac.jp

- [1] T. Kimura et al., Nature **426**, 55 (2003).
- [2] T. Kimura et al., Phys. Rev. B **68**, 060403(R) (2003).
- [3] T. Goto et al., Phys. Rev. Lett. **92**, 257201 (2004).
- [4] T. Arima et al., Phys. Rev. B **72**, 100102 (2005).
- [5] G. Lawes et al., Phys. Rev. Lett. **95**, 087205 (2005).
- [6] L. C. Chapon et al., Phys. Rev. Lett. **93**, 177402 (2004).
- [7] G. R. Blake et al., Phys. Rev. B **71**, 177402 (2004).

- [8] T. Kimura, G. Lawes , and A. P. Ramirez, Phys. Rev. Lett.**94**, 137201 (2005).
- [9] M. Kenzelmann et al.,Phys. Rev. Lett.**95**,087206 (2005).
- [10] H. Katsura, N. Nagaosa, and A.V.Balatsky, Phys. Rev. Lett. **95**,057205 (2005).
- [11] Y. Aharonov and A. Casher,Phys. Rev. Lett.**53**, 319(1984).
- [12] A. V. Balatsky and B. L. Altshuler, Phys. Rev. Lett. **70**, 1678 (1993).
- [13] I. Dzyaloshinskii, J. Phys. Chem. Solids **4**, 241 (1958); T. Moriya, Phys. Rev. **120**, 91 (1960).
- [14] M. Mostovoy, cond-mat/0510692.
- [15] I.A. Sergienko, E. Dagotto, cond-mat/0508075.
- [16] T. Nagamiya, in *Solid State Physics*, edited by F. Seitz, D. Turnbull, and H. Ehrenreich (Academic Press, New York, 1967), Vol.20, p.305.
- [17] We should note here that we have neglected high-frequency correlations such as $\langle S_{2Q} S_0 \rangle$, since the modes $S_{\pm 2Q}^\alpha$ have an energy higher than that of S_0^α or $S_{\pm Q}^\alpha$.
- [18] S. Foner, *Magnetism I*, edited by G. T. Rado and H. Suhl, (Academic Press, New York and London, 1963) p.383.
- [19] R. Kajimoto *et al*, J. Phys. Soc. Jpn. **74**, 2430 (2005).
- [20] M. Tovar *et al.*, Phys. Rev. B**60**, 10199 (1999).
- [21] A. Pimenov *et al.*, to appear in Nature Physics(cond-mat/0602173).